

Characterization of self-injected electron beams from LWFA experiments at SPARC LAB

G. Costa^a, M. P. Anania^a, F. Bisesto^a, E. Chiadroni^a, A. Cianchi^b, A. Curcio^c, M. Ferrario^a, F. Filippi^a, A. Marocchino^a, F. Mira^a, R. Pompili^a, A. Zigler^d

^aLaboratori Nazionali di Frascati, INFN, Via E. Fermi, 40, 00044 Frascati, Italia

^bUniversity of Rome Tor Vergata, Via della Ricerca Scientifica, 1, 00133 Roma, Italia

^cUniversity of Rome La Sapienza, Piazzale Aldo Moro, 5, 00185 Roma, Italia

^dRacah Institute of Physics, Hebrew University, 91904 Jerusalem, Israel

Abstract

The plasma-based acceleration is an encouraging technique to overcome the limits of the accelerating gradient in the conventional RF acceleration. A plasma accelerator is able to provide accelerating fields up to hundreds of GeV/m , paving the way to accelerate particles to several MeV over a short distance (below the millimetre range).

Here the characteristics of preliminary electron beams obtained with the self-injection mechanism produced with the FLAME high-power laser at the SPARC LAB test facility are shown.

In detail, with an energy laser on focus of $1.5 J$ and a pulse temporal length (FWHM) of $40 fs$, we obtained an electron plasma density due to laser ionization of about $6 \times 10^{18} cm^{-3}$, electron energy up to $350 MeV$ and beam charge in the range $(50 - 100) pC$.

1. Introduction

Particle accelerators are nowadays used in a wide range of fields: they are the fundamental tools for elementary particle research and high-energy physics in general, but at the same time they are an important resource employed in several other areas, from medicine to the industry [1].

The goal of the acceleration of charged particles has been to continually achieve higher energies and, due to limitations on the maximum electric fields that can be obtained by conventional techniques, ever larger accelerator systems have become necessary, so the cost of such systems is so huge that multinational collaboration and construction over many years is required. In fact, RF structures can sustain accelerating fields up to $100 MV/m$, limited by breakdown, therefore, hundreds-of-metres-long machines are needed to achieve beams at GeV scale.

In 1979, Tajima and Dawson proposed a new method to accelerate charged particles using laser-plasma interaction (Laser WakeField Acceleration, LWFA) [2]. With this technique, a short laser pulse interacts with a plasma generating a strong oscillating electrostatic field in its wake. The novelty of this technique is that the electrostatic fields generated by such a process can

be several orders of magnitude larger than that which can be generated by conventional radio frequency cavities in accelerators. Indeed, the plasma accelerating field scales as $E_0[V/m] \simeq 96 \sqrt{n_0[cm^{-3}]}$, where n_0 is the electron plasma density [3]. Therefore, accelerating gradients up to TeV/m are achievable. In the last ten years, thanks to the implementation of the Chirped Pulse Amplification (CPA) method [4], the development of TW -class fs -level lasers has been fundamental to study LWFA [5] and electron beams with energy at GeV -scale have been experimentally produced [6, 7, 8, 9].

Our experiment about the characterization of preliminary electron beams, produced by self-injection at the SPARC LAB test facility [10] (INFN-LNF) by using the ultra-short high power laser FLAME [11], is placed in this context. The latter is a CPA Ti:Sa laser system, a compact femtosecond laser source, providing up to $7.5 J$ pulse energy at $10 Hz$ repetition rate, with a bandwidth of $80 nm$ and a contrast ratio in the order of 10^{10} . The pulse can be as low as $25 fs$ and leads to a peak power higher than $250 TW$. The goal of our experimental work was to reproduce the strongly non-linear regime, therefore extremely relativistic laser intensities, testing our experimental set-up and confirming our spe-

cific simulation.

2. Experimental parameters and simulations

To reproduce the strongly non-linear bubble regime, the main laser pulse parameters were fixed according to the scaling laws for laser wakefield accelerators [12, 13]: the energy pulse was within the values $E = (1 - 1.5) J$, delivered in $\tau_L = (35 - 40) fs$ temporal length (see Fig.1), over a $10 \mu m/e^2$ radius on focus (see Fig. 2). In this way we had a laser intensity $I_0 = 2E_0/\tau_L\pi r^2 \approx 2 \times 10^{19} W/cm^2$, therefore the laser normalized intensity [3, 12] is $a_0 \approx 0.855 \times 10^{-9} \lambda_L \sqrt{I_0} \approx 3.3$, confirming the strongly non-linear regime.

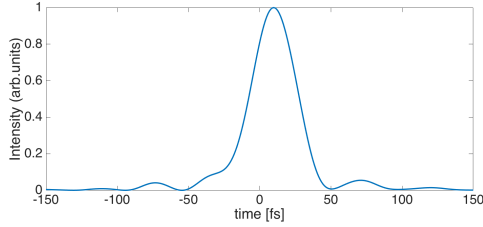


Figure 1: FLAME temporal pulse length measurement made using the APE SPIDER after the compression.

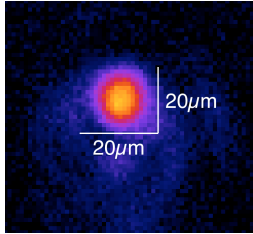


Figure 2: FLAME focal spot in vacuum at the gas-jet position, obtained by means of a Basler Scout scA640-70gm CCD camera equipped with a microscope objective.

To reach the maximum electron beam energy, given by $E_b = 2m_e c^2 a_0 n_c / 3n_e$, where $n_c = \pi/r_e \lambda_L^2$ is the critical plasma density, r_e is the Rayleigh length and $\lambda_L = 800 nm$ is the laser wavelength, it is necessary to set the acceleration length L_{acc} to the dephasing length: $L_{acc} = L_{deph} = (2/3\pi) \sqrt{a_0 \lambda_L} (n_c/n_e)^{3/2}$, while the pump depletion length $L_{depl} \approx c\tau_L (n_c/n_e) \geq L_{deph}$. In this way, for a given a_0 , a longer pump depletion length, corresponding to a longer dephasing length, is due to an increase of the critical density, which indicates a decrease of the electron self-injection threshold into the laser wakefield as well as a decrease of the critical power for the self-guiding [13].

Our regime of interaction was confirmed also by full 3D PIC simulations (see Fig. 3), performed with the ALaDyn code [14, 15, 16] for a driver laser pulse and a background electron plasma density with about the same characteristics of the experimental ones. The code predicted polyenergetic electron beams, with energies and energy spreads both consistent with the measurements [17].

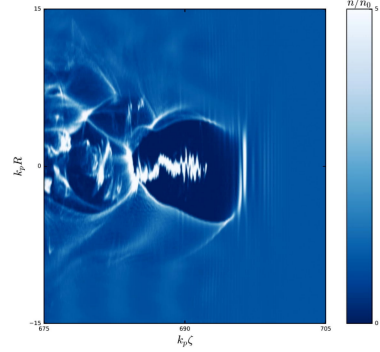


Figure 3: Example of a 2D plasma density plot from PIC Code ALaDyn simulations, in dimensionless units. The snapshot is taken at $0.7 mm$ propagation distance, the laser FWHM duration is $30 fs$, while the initial laser diameter is $11.76 \mu m$. For the full 3D simulation it was used a $1120 \times 304 \times 304$ moving window, with a longitudinal resolution of $0.05 \mu m$, a transverse resolution of $0.0125 \mu m$ and 8 particles per cell. The plasma density is normalized to the unperturbed background density ($n_e = 1 \times 10^{19} cm^{-3}$) [17].

3. Experimental set-up and results

The laser was focused by means of an off-axis parabolic (OAP) mirror with $1 m$ focal length in the middle of the vacuum ($10^{-6} mbar$) interaction chamber on a specific *He* gas-jet target. Outside the vacuum chamber was placed a gas bottle equipped with a specific knob used to throw gas with variable pressure ($0 - 50 bar$). The gas-jet nozzle, displayed in Fig. 4, has been designed to provide a supersonic gas profile, which obtained a sharp boundary with the vacuum. The flow of gas into the vacuum was optimized and minimized using a solenoid valve that was normally closed, the gas was injected synchronously with the laser pulse so that when the laser arrived into the chamber, it could ionize the gas and bring it into the state of plasma.

The experimental set-up, shown in Fig. 5, was composed by a Mach-Zehnder interferometer to measure the generated plasma density, a LANEX screen scintillator to detect the electron bunch transverse dimensions, a Fuji BAS Imaging Plate (IP) with a specific Durr CR35 Bio scanner to evaluate the electron bunch charge, and

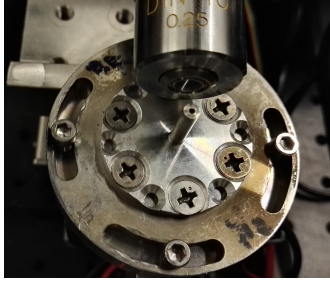


Figure 4: FLAME supersonic gas-jet, the design of the nozzle allows to obtain a gas column with a sharp edge.

a 1 T permanent dipole coupled to another LANEX screen scintillator oriented at 60° with respect to the direction of the beam propagation to obtain the electron energy spectrum.

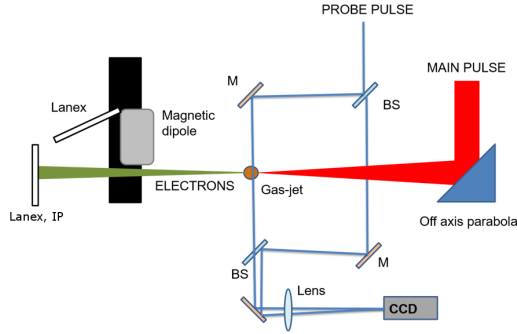


Figure 5: Self-injection experimental set-up composed by a Mach-Zehnder interferometer for plasma density measurement (where BS: Beam Splitter, M: Mirror), a magnetic spectrometer for electron energy measurement, a LANEX screen and an IP for electron bunch transversal dimensions and charge.

3.1. Plasma density and acceleration length

The Mach-Zehnder interferometer uses the dependence of the plasma refraction index $\eta = \sqrt{1 - n_e/n_c}$ on the medium density, and its variation can be obtained measuring the phase shifting of a propagating beam. For this purpose, we used a probe beam (10% fraction of the main beam), that was split in two arms, while only one was passing through the plasma. Observing their recombination, we were able to look at the image of the plasma channel through a 25 cm focal length lens, while the interferogram was collected by a Basler Scout 750 CCD camera (see Fig. 6). The dephasing of the interference fringes, due to the transit through the plasma, was analysed with a specific Matlab GUI program, which reconstructs the phase map obtained by the shift of the fringes recorded [18].

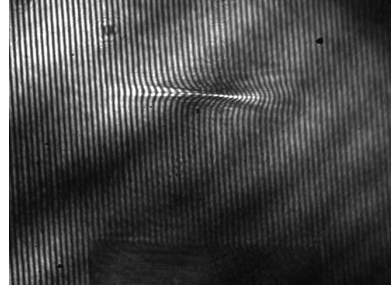


Figure 6: Typical interferogram in the presence of plasma. The spatial calibration has been performed by using the shadow of the gas-jet, whose thickness is known.

The electron plasma density obtained was $n_e \approx (6 - 8) \times 10^{18} \text{ cm}^{-3}$, and the maximum acceleration length, measured looking at the extension of the plasma in the interferometric images of the laser propagated through the plasma, was in the range $L_{acc} = (1 - 2) \text{ mm}$, according to the diameter of the gas-nozzle and of the plasma density used shot by shot [17].

Using these experimental measurements, it was possible to calculate the maximum electric field reached in the plasma, that was $E_0 \approx 240 \text{ GV/m}$, considering a plasma density equal to $6 \times 10^{18} \text{ cm}^{-3}$, value confirmed by the fact that the bubble radius is $R_{bubble} = 2\sqrt{a_0}c/\omega_p \approx \lambda_p/2$, where $\omega_p \approx e\sqrt{n_0/(\epsilon_0 m_e)}$ is the plasma frequency and $\lambda_p = 2\pi c/\omega_p$ [3].

In this way, for our parameters, we could notice that for an acceleration length, measured as the plasma channel length, as low as $L_{acc} = 1.5 \text{ mm}$, we obtained $L_{acc} < L_{deph} \approx 1.55 \text{ mm} < L_{depl} \approx 3.5 \text{ mm}$, and reached the maximum energy gain $E_b \approx 330 \text{ MeV}$ for our system.

The channel length was also measured by images recorded using 90° Thomson scattering diagnostic, which provided on-line data of the electron-photon collisions, due to the interaction between plasma and the laser pulse, used also to check the best conditions for electron acceleration. It was set up with a 200 mm focal length lens, which provided the possibility to get, on the CCD camera (Basler scA1600-14gc), a magnified image of the region of interest, and a 35 mm objective [19].

3.2. Electron bunch dimensions, charge and energy

Measurements of electron beam transverse profile were performed with the LANEX screen, placed 50 cm far from the source, outside the experimental chamber at 90° with respect to the direction of the electrons, i.e. the propagation direction of the laser pulse. A CCD camera (Basler scA640-70gm), looking at the screen, has been

used to image it. A typical profile is in Fig. 7: the dimension of the obtained electron spot was in the range $(1 - 3) \text{ mm}$ FWHM, which corresponds to a divergence in the range $(2 - 6) \text{ mrad}$.

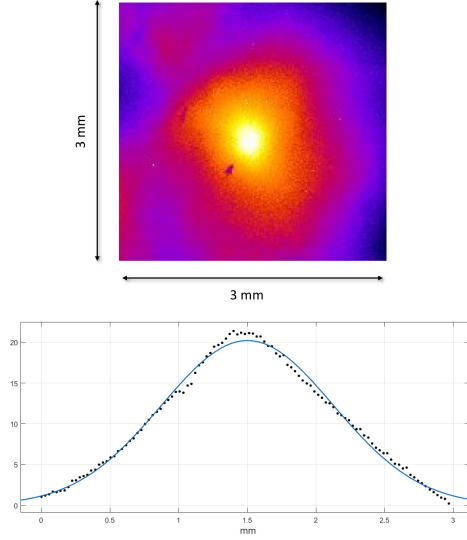


Figure 7: Typical measurement of electron beam transverse profile. Axes are Intensity [arb. units] vs dimension [mm]; data (black dots), fit (blue curve).

By replacing this LANEX screen with an IP and reading it with our Durr scanner, we were able to retrieve the deposited electron radiation through the Gray Value data shown in Fig. 8. It was then converted in PSL (photostimulated luminescence) via the calibration presented in the work [17, 20, 21], leading us to an evaluation of the charge typically in the range $(50 - 100) \text{ pC}$. The charge data confirmed the electron beam transversal information found with the LANEX screen.

Simulations made with the General Particle Tracer (GPT) software [22] were used to optimize the magnetic spectrometer setup in order to measure the electron energy and to find the right correlation between screen position and electron energy [19]. The values obtained were in the range $(150 - 350) \text{ MeV}$ (Fig. 9), with an energy spread of about $(10 - 15)\%$, therefore measurements consistent with the expected maximum energy gain E_b .

4. Conclusions and future developments

Experimental results about the characterization of preliminary electron beams, produced by the self-injection bubble regime at SPARC-LAB have been shown. Electrons produced with the FLAME laser were

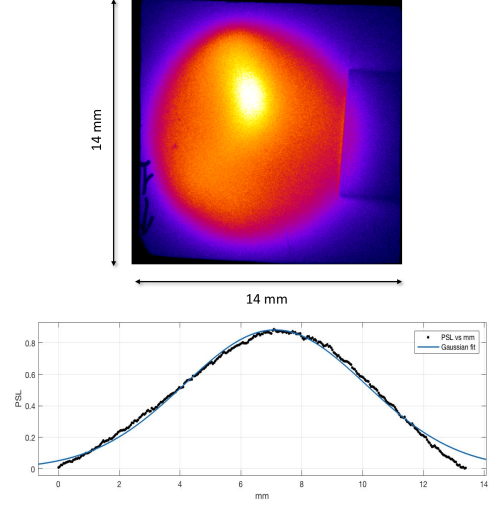


Figure 8: Typical measurement of IP spot and converted integrated profile. Axes are PSL vs dimension [mm]; data (black dots), fit (blue curve).

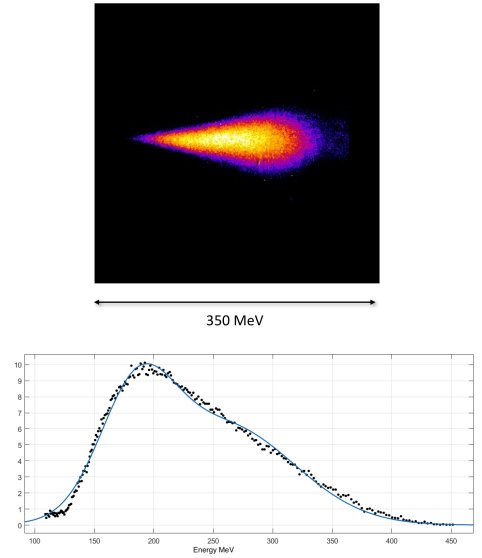


Figure 9: Typical electron energy spectrum measurement. Axes are Intensity [arb. units] vs Energy [MeV]; data (black dots), fit (blue curve).

mainly used to perform diagnostic tests, based on betatron [23, 24] and optical transition radiation [25, 26, 27].

In the near future, we are developing a magnetic transport line for the electrons coming from the plasma source, in order to better control them. In particular, we are designing a particle selector to keep only the energetic core of the beam and a magnetic triplet to control the electron divergence, typically high in a plasma accelerator, and tune the bunch transverse beam size. Moreover, an integrated current transformer (ICT) will be installed in the target area to measure the electron charge. On the other side, an optimized injection method will be studied to reduce the energy spread. In particular, an experiment based on external injection scheme is foreseen, combining the high brightness SPARC-LAB photoinjector and the FLAME laser [28, 29, 30].

Acknowledgements

This work was supported by the European Union's Horizon 2020 research and innovation programme under grant agreement No. 653782.

References

References

- [1] S. Eliezer, K. Mima, Applications of Laser-Plasma Interactions, CRC Press, 2008.
- [2] T. Tajima, J. Dawson, Laser electron accelerator, Physical Review Letters 43 (4) (1979) 267.
- [3] E. Esarey, C. Schroeder, W. Leemans, Physics of laser-driven plasma-based electron accelerators, Reviews of Modern Physics 81 (3) (2009) 1229.
- [4] D. Strickland, G. Mourou, Compression of amplified chirped optical pulses, Optics communications 55 (6) (1985) 447–449.
- [5] A. Pukhov, S. Gordienko, S. Kiselev, I. Kostyukov, The bubble regime of laser-plasma acceleration: monoenergetic electrons and the scalability, Plasma physics and controlled fusion 46 (12B) (2004) B179.
- [6] C. Geddes, C. Toth, J. Van Tilborg, E. Esarey, C. Schroeder, D. Bruhwiler, C. Nieter, J. Cary, W. Leemans, High-quality electron beams from a laser wakefield accelerator using plasma-channel guiding, Nature 431 (7008) (2004) 538–541.
- [7] W. P. Leemans, B. Nagler, A. J. Gonsalves, C. Tóth, K. Nakamura, C. G. Geddes, E. Esarey, C. Schroeder, S. Hooker, GeV electron beams from a centimetre-scale accelerator, Nature physics 2 (10) (2006) 696–699.
- [8] M. Fuchs, R. Weingartner, A. Popp, Z. Major, S. Becker, J. Osterhoff, I. Cortie, B. Zeitler, R. Hürlein, G. D. Tsakiris, et al., Laser-driven soft-x-ray undulator source, Nature physics 5 (11) (2009) 826–829.
- [9] S. P. Mangles, C. Murphy, Z. Najmudin, A. G. R. Thomas, J. Collier, A. E. Dangor, E. Divall, P. Foster, J. Gallacher, C. Hooker, et al., Monoenergetic beams of relativistic electrons from intense laser-plasma interactions, Nature 431 (7008) (2004) 535–538.
- [10] M. Ferrario, D. Alesini, M. Anania, A. Bacci, M. Bellaveglia, O. Bogdanov, R. Boni, M. Castellano, E. Chiadroni, A. Cianchi, et al., Sparc_lab present and future, Nuclear Instruments and Methods in Physics Research Section B: Beam Interactions with Materials and Atoms 309 (2013) 183–188.
- [11] F. G. Bisesto, M. P. Anania, E. Chiadroni, A. Cianchi, G. Costa, A. Curcio, M. Ferrario, F. Filippi, R. Pompili, A. Zigler, The flame laser at sparc lab, these proceedings.
- [12] A. Pukhov, J. Meyer-ter Vehn, Laser wake field acceleration: the highly non-linear broken-wave regime, Applied Physics B: Lasers and Optics 74 (4) (2002) 355–361.
- [13] T. Tajima, G. Mourou, K. Nakajima, Laser acceleration, Riv. Nuovo Cim. 40 (2017) 1.
- [14] C. Benedetti, A. Sgattoni, G. Turchetti, P. Londrillo, Aladyn: A high-accuracy pic code for the maxwell-vlasov equations, IEEE Transactions on plasma science 36 (4) (2008) 1790–1798.
- [15] P. Londrillo, C. Benedetti, A. Sgattoni, G. Turchetti, Charge preserving high order pic schemes, Nuclear Instruments and Methods in Physics Research Section A: Accelerators, Spectrometers, Detectors and Associated Equipment 620 (1) (2010) 28–35.
- [16] A. Marocchino, et al., Design of high brightness plasma wake-field acceleration experiment at sparc lab test facility with the 3d particle-in-cell aladyn, these proceedings.
- [17] A. Curcio, M. Anania, F. Bisesto, E. Chiadroni, A. Cianchi, M. Ferrario, F. Filippi, D. Giulietti, A. Marocchino, F. Mira, et al., First measurements of betatron radiation at flame laser facility, Nuclear Instruments and Methods in Physics Research Section B: Beam Interactions with Materials and Atoms.
- [18] F. F. Plasma source characterization for plasma-based acceleration experiments (2017).
- [19] B. F. Coherent light sources and optical techniques for thomson scattering and laser-plasma experiments. (2017).
- [20] A. Curcio, P. Andreoli, M. Cipriani, G. Claps, F. Consoli, G. Cristofari, R. De Angelis, D. Giulietti, F. Ingenito, D. Pacella, Imaging plates calibration to x-rays, Journal of Instrumentation 11 (05) (2016) C05011.
- [21] N. Nakanii, K. Kondo, S. Suzuki, T. Kobayashi, T. Asaka, K. Yanagida, K. Tsuji, K. Makino, T. Yamane, T. Yabuuchi, et al., Absolute calibration of imaging plate for electron spectrometer measuring gev-class electrons, in: Journal of Physics: Conference Series, Vol. 112, IOP Publishing, 2008, p. 032073.
- [22] M. De Loos, S. Van der Geer, General particle tracer: A new 3d code for accelerator and beamline design, in: 5th European Particle Accelerator Conference, 1996, p. 1241.
- [23] A. Curcio, M. Anania, F. Bisesto, E. Chiadroni, A. Cianchi, M. Ferrario, F. Filippi, D. Giulietti, A. Marocchino, M. Petrarca, et al., Trace-space reconstruction of low-emittance electron beams through betatron radiation in laser-plasma accelerators, Physical Review Accelerators and Beams 20 (1) (2017) 012801.
- [24] A. Curcio, M. Anania, F. Bisesto, E. Chiadroni, A. Cianchi, M. Ferrario, F. Filippi, D. Giulietti, A. Marocchino, F. Mira, et al., Single-shot non-intercepting profile monitor of plasma-accelerated electron beams with nanometric resolution, Applied Physics Letters 111 (13) (2017) 133105.
- [25] F. Bisesto, M. P. Anania, M. Botton, E. Chiadroni, A. Cianchi, A. Curcio, M. Ferrario, M. Galletti, R. Pompili, E. Schleifer, et al., Novel single-shot diagnostics for electrons from laser-plasma interaction at sparc_lab, Quantum Beam Science 1 (3) (2017) 13.
- [26] F. Bisesto, M. P. Anania, A. Cianchi, E. Chiadroni, A. Curcio, M. Ferrario, R. Pompili, A. Zigler, Innovative single-shot diagnostics for electrons from laser wakefield acceleration at flame, in: Journal of Physics: Conference Series, Vol. 874, IOP Publishing, 2017, p. 012035.

- [27] F. Bisesto, M. Anania, E. Chiadroni, A. Cianchi, G. Costa, A. Curcio, M. Ferrario, M. Galletti, R. Pompili, E. Schleifer, et al., Innovative single-shot diagnostics for electrons accelerated through laser-plasma interaction at flame, in: SPIE Optics+ Optoelectronics, International Society for Optics and Photonics, 2017, pp. 102400K–102400K.
- [28] F. Bisesto, M. Anania, A. Bacci, M. Belleveglia, E. Chiadroni, A. Cianchi, A. Curcio, D. Di Giovenale, G. Di Pirro, M. Ferrario, et al., Laser–capillary interaction for the exin project, Nuclear Instruments and Methods in Physics Research Section A: Accelerators, Spectrometers, Detectors and Associated Equipment 829 (2016) 309–313.
- [29] A. Rossi, M. Anania, A. Bacci, M. Belleveglia, F. Bisesto, E. Chiadroni, A. Cianchi, A. Curcio, A. Gallo, D. Di Giovenale, et al., Stability study for matching in laser driven plasma acceleration, Nuclear Instruments and Methods in Physics Research Section A: Accelerators, Spectrometers, Detectors and Associated Equipment 829 (2016) 67–72.
- [30] A. R. Rossi, A. Bacci, M. Belleveglia, E. Chiadroni, A. Cianchi, G. Di Pirro, M. Ferrario, A. Gallo, G. Gatti, C. Maroli, et al., The external-injection experiment at the sparc_lab facility, Nuclear Instruments and Methods in Physics Research Section A: Accelerators, Spectrometers, Detectors and Associated Equipment 740 (2014) 60–66.